MALDI/TOF/MS and SEC Study of Astromol Dendrimers Having Cyano End Groups

Lujia Bu, William K. Nonidez, and Jimmy W. Mays*

Department of Chemistry, University of Alabama at Birmingham, Birmingham, Alabama 35294

Nora Beck Tan

Polymers Research Branch, U.S. Army Research Laboratory, APG, Maryland 21005-5096

Received March 30, 1999; Revised Manuscript Received April 6, 2000

ABSTRACT: Matrix-assisted laser desorption/ionization time-of-flight mass spectrometry (MALDI/TOF/MS), size exclusion chromatography (SEC), and dilute solution viscometry were used to analyze the structure of three generations of Astromol (trademark of DSM) dendrimers having cyano end groups. The molecular weights, the defect contents, and the structures of the "imperfect" dendrimers were determined by MALDI/TOF/MS analysis with fractions collected using a SEC fraction collector. The peak broadening observed for these materials in SEC was studied by adding different co-solvents to the SEC mobile phase. The hydrodynamic radius of the dendrimers was measured both by dilute solution viscometry and by SEC universal calibration. Our radii data are comparable to previously published results for these dendrimers obtained by neutron scattering and support the opinion that dendrimers have compact spherical structures.

Introduction

Dendrimers are produced by controlled, repetitive reaction sequences. There are two basic synthetic strategies for preparing these macromolecules: a divergent approach[1,2] and a convergent approach.[3] Interest in these molecules is due to their unique structure and physical behavior.[4,5] An excellent recent review on dendrimers has been published by Meijer and coworkers.[6] Following the first synthesis of dendrimers, molecular characterization studies on dendrimers of different chemistries were reported using size exclusion chromatography (SEC), viscometry, ^{1}H and ^{13}C NMR (nuclear magnetic resonance spectroscopy), and scattering methods.[7−10] However, many theoretical calculations and mathematical simulations on dendrimer behavior are yet to be rigorously tested.[11−14]

In this study, the molecular characteristics and dilute solution properties of three generations (generations 3, 4, and 5) of poly(propyleneimine) dendrimers with cyano end groups were investigated by means of SEC, intrinsic viscosity measurements, and matrix-assisted laser desorption/ionization time-of-flight mass spectrometry (MALDI/TOF/MS). The advantage of MALDI/TOF/MS as a method for dendrimer molecular weight determination is that, provided molecular weight is not too high, it provides much better mass resolution than traditional polymer characterization methods such as SEC. Also, the selection of solvent is not as critical as for SEC and other solution characterization methods.

Experimental Section

Materials. The poly(propyleneimine) dendrimers with cyano end groups used in this study (generations 3, 4, and 5) were obtained from DSM Fine Chemicals (Heerlen, The Netherlands), under their trade name of Astromol. The solubility of the resulting dendrimers depends on the type of end group. Cyano end groups allow these dendrimers to be dissolved in tetrahydrofuran (THF), the most common solvent for SEC.

Size Exclusion Chromatography. The SEC chromatograms were obtained with a custom assembled Waters SEC system operating at room temperature. The system was built with a Waters 515 pump and a Waters 410 refractive index (RI) detector. It was equipped with a four-column bank of cross-linked polystyrene gel columns with pore sizes of 500, 10^3 A, HR SE (Waters Association, Milford, MA) and a 5 mm linear column from American Polymer Standards. THF was used as the mobile phase and for making polymer solutions for SEC analysis. A nominal flow rate setting of 1.0 mL/min and injection volumes of 200 μL of 0.02−0.3% (g/mL) solutions were used.

Deposition of SEC Fraction. An Advantec SF-2120 fraction collector (Advantec Toyo Kaisha Ltd., Japan) was used to deposit eluting polymer fractions directly onto the MALDI target plate. The fraction collector was positioned at the outlet of the SEC columns in parallel with the RI detector. A flow splitter was placed before the RI detector and fraction collector to allow the SEC eluent to pass through both sides at the same rate. The flow rate was adjusted by the injection of 9-anthracenemethanol. By comparing the maximum intensity of fractions deposited on a thin layer plate and the peak of the RI signal, the time delay between the two detectors was determined. The flow rate was adjusted to be equal on both sides of the parallel arrangement (0.5 mL/min).

MALDI Sample Preparation. *trans*-3-Indoleacrylic acid (IAA) was used as matrix and THF as the solvent in these experiments. When the fraction collector was used, the matrix was spotted on the plate followed by the spotting of dendrimer fractions. When unfractionated dendrimers were directly analyzed by MALDI/TOF/MS, matrix and dendrimers were dissolved together in THF prior to spotting onto the sample plate. The solution concentrations used for both the matrix and polymers in the MALDI/TOF/MS method were based upon rather standard conditions: 0.1 mmol of matrix and 0.2 nmol of polymer were spotted into round wells of area of ca. 7 mm^2. The amount of solution used was 1 μL, withdrawn by an Eppendorf micropipet. The matrix and sample concentrations were not the critical control factors for obtaining high-quality spectra.

MALDI/TOF/MS Instrument. A PerSeptive Biosystems (Framingham, MA) Voyager Elite MALDI/TOF mass spectrometer was used to obtain the mass spectra. The system is equipped with a N_2 laser providing 337 nm, 3 ns wide pulses with the accelerating voltage variable up to 25 kV. Delayed extraction mode was applied in both linear and reflectron time-

10.1021/ma990458p CCC: $19.00
Published on Web 05/20/2000

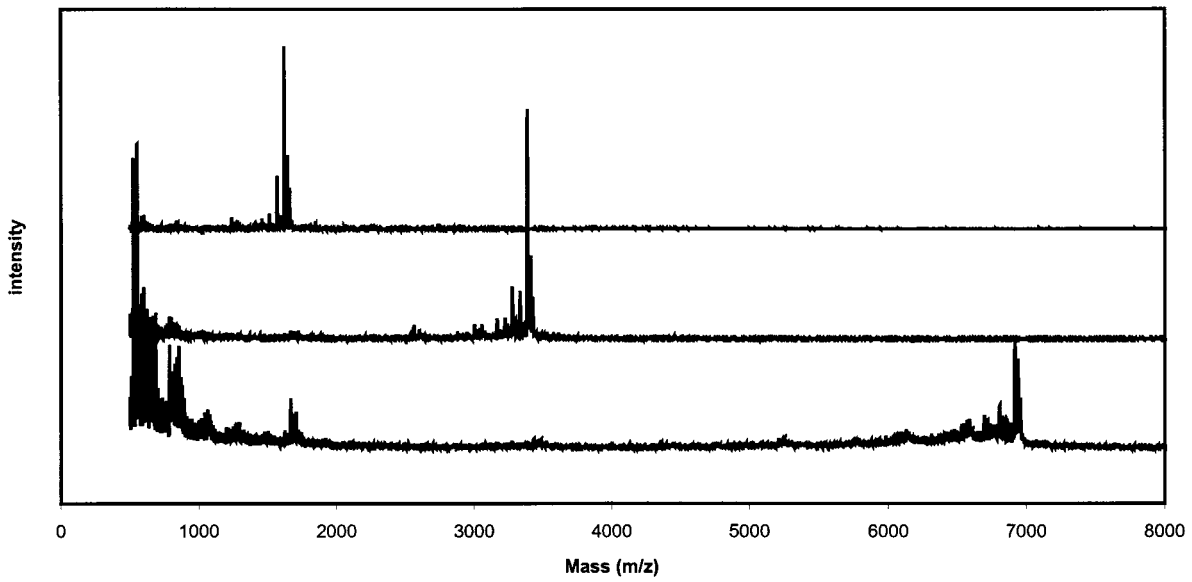

Figure 1. MALDI/TOF/MS of DSM dendrimers of different generations without fractionation. From top to bottom: CN-64, CN-32, and CN-16.

of-flight detection systems. The instrument is equipped with electron multiplier detectors having a theoretical detection limit up to 300 000 mass units. A low mass gate was used to avoid detector saturation from high-intensity low mass ions and fragments. The theoretical mass accuracy is ±0.05% with external calibration under linear mode and when delayed extraction is applied; these were the conditions used in this work. The experimental parameters such as acceleration voltage, grid voltage, guide wire voltage, and delay time were optimized to obtain high-resolution spectra. The instrument was calibrated externally using Angiotensin I (m = 1296.69) and Insulin B chain (m = 3496.96). The calibration standards (aqueous solution) were mixed with IAA/THF matrix and deposited on the wells beside the sample wells. The instrument was calibrated just before the measurements to keep the experimental conditions exactly the same.

Dilute Solution Viscosity. Viscosity measurements on DSM dendrimers were performed in THF in an Ubbelohde viscometer at 25 °C. The intrinsic viscosity [η] was determined by extrapolation of η_{sp}/c to infinite dilution. (Here η_{sp} is the specific viscosity and c is polymer concentration.) The hydrodynamic radius R_h was calculated from the intrinsic viscosity in the usual way (by applying the Stokes−Einstein equation).

Results and Discussion

MALDI/TOF Mass Spectra of Astromol Dendrimers of Different Generations without Fractionation. The different generations of DSM dendrimers, in THF solution with IAA matrix, were deposited on the sample plate directly, without SEC fractionation. The spectra (Figure 1) show that the dendrimers are narrowly dispersed but clearly not monodisperse. The polydispersity mainly reflects the absence of branches on the shell. The higher the generation number, the broader the distribution.

The theoretical molecular weight of a dendrimer of generation g is[1]

$$M_g = M_c + N_c\left[M_{BC}\left(\frac{N_b^g - 1}{N_b - 1}\right) + M_t N_b^g\right] \qquad (1)$$

where M_c, M_{BC}, and M_t are core, branch cell, and terminal unit molecular weights, respectively. N_c is core multiplicity, and N_b is branch-juncture multiplicity. On the basis of the known mass accuracy of 0.05% and considering the masses of these dendrimers, their masses could be measured by MALDI/TOF/MS to within about 1−3 Da, depending on molecular weight. In the MALDI/TOF/MS spectra of these dendrimers, the main peaks of the spectra are singly charged molecular ions. The measured molecular weights for the dendrimers of three different generations, and their theoretical molecular weights, are listed in Table 1. From Table 1, we can see that the molecular weights obtained from the measurements are, within experimental error, in agreement with theoretically calculated values. Clearly, the MALDI/TOF/MS method gives very accurate molecular weight information. Similar results were obtained by electrospray mass spectrometry (ESI-MS).[15] Unlike ESI-MS, which generates multiple charge ions, ions generated by MALDI/TOF/MS are predominantly singly charged. Thus, spectral deconvolution is not necessary, and MALDI/TOF/MS provides true mass and mass distribution information directly.

Table 1. Molecular Weights of Dendrimers with Different Generations Compared with the Theoretical Mass and Standard Deviation (All in daltons)

	CN-16	CN-32	CN-64
theoretical mass	1622.31	3384.9	6909.9
MALDI measurement[a]	1621.65	3386.1	6911.4
standard deviation[b]	0.07	0.1	0.6
mass accuracy, ±0.05%[c]	0.81	1.7	3.5

[a] Molecular weight of dendrimer after subtracting the mass of the ionizing species. [b] Experimental precision based upon 10 measurements in the same sample well for each specimen. [c] Theoretical mass accuracy for external calibration in linear mode is 0.05%.

In addition to the main peaks in the spectra shown in Figure 1, there are many peaks at lower molecular weights that have lower intensities. These lower intensity peaks may reflect the response of impurities or species ionized by different ions (protons versus sodium versus potassium). Sodium and potassium abducted molecular ions can be easily distinguished from the protonated ions since they are 22 and 38 mass units higher. Theoretically, there are two unwanted reactions during the synthesis of these dendrimers as described be Meijer et al.[6,15] One is "missed" Michael additions

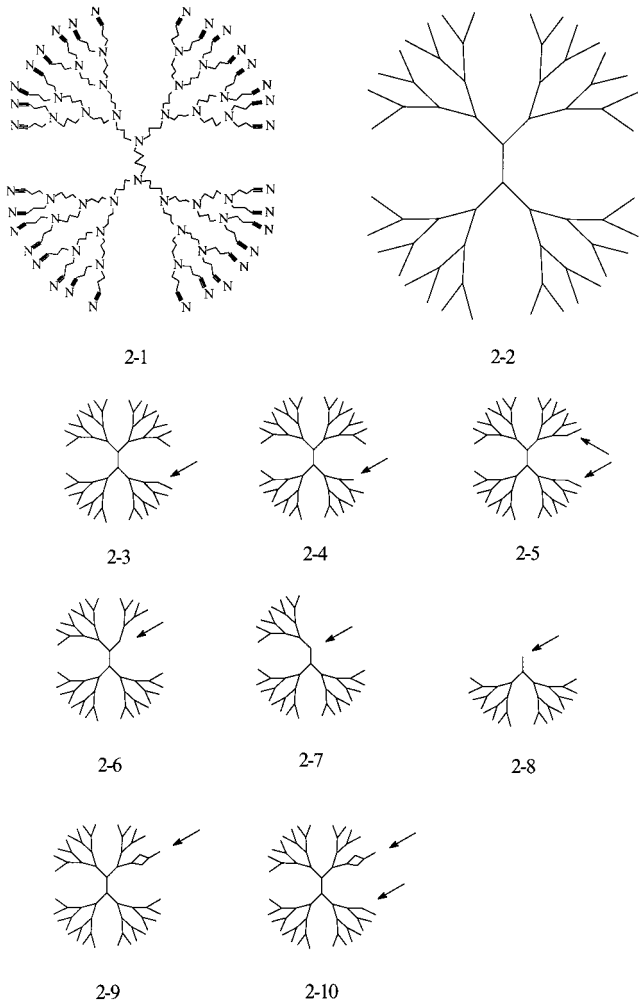

Figure 2. Interpretation of MALDI/TOF spectra in terms of the most prominent structures of CN-32 and its impurities. 2-1: perfect dendrimer structure of CN-32. 2-2: a skeletal sketch of the CN-32 perfect dendrimer. 2-3 to 2-8 illustrate type 1 defects: CN-32 with one branch missing in 2-3; two branches missing from the same amine in 2-4; two branches missing from different amines in 2-5; $^{7}/_{8}$ dendrimer in 2-6; $^{3}/_{4}$ dendrimer in 2-7; and $^{1}/_{2}$ dendrimer in 2-8. 2-9 shows type 2 defects. 2-10 shows type 1 and type 2 defects in the same dendrimer.

leading to "missing branches" (type 1 defect), and another is cyclization (type 2 defect). Their typical structures, shown in Figure 2, can be anticipated on the basis of the chemistry used in their synthesis. Both types of defects will lead to characteristic molecular weight patterns. For example, in the case of type 1 impurities, molecular weights of CN-32 are 3331.8 when one branch is missing and 3274.7 when two branches are missing. The molecular weights are 3155.6 and 2926.3 in the case of cyclic reactions. The signals from these fragments should be clearly evident in the MALDI spectra. On the basis of the above known side reactions and by consideration of the possible structures and their calculated molecular weights and correlation with peaks observed in the spectrum, we can assign most of the MALDI fragments observed for CN-32, as shown in Figure 2. Sodium and potassium ion peaks can be easily distinguished from the protonated peaks because they are spaced regularly with distinct mass differences relative to protonated ions. Upon assignment, we found that the occurrence of type 2 reactions is very rare, if it exists at all. All the secondary peaks can be assigned to type 1 reactions without exception down to a mass number of 2800 (Table 2). By linking peak points corresponding to protonated species together (Figure 3), we find that the peak height decays exponentially as the number of missing branches increases. Two separate curves were drawn to fit data corresponding to missing odd number of branches and missing even numbers of branches. The curves (Figure 3) are very smooth with the exception of the peak representing seven missing (H-7) branches. The intensity of this peak is much greater than the intensities of peaks corresponding to specimens that are missing fewer numbers of branches. We believe that this H-7 peak corresponds to imperfect dendrimers that lack $^{1}/_{8}$ of the mass of the perfect dendrimer (so-called $^{7}/_{8}$ dendrimer; see Figures 2-6). If this is true, it seems likely that peaks for similar structures with more branches missing can be found in the spectrum. Indeed, we find mass fragments of 1721.8 and 2563.7 in the spectrum closely matching the theoretical masses of 1718.4 for half dendrimer and 2560.7 for $^{3}/_{4}$ dendrimer (Figures 2-7 and 2-8). By connecting these points, a third trend line that also shows exponential decay can be obtained. Even though the molecular weights of these fragments are well below those of the major component (the perfect dendrimer), they can still be assigned as fragments of the same generation. They do not represent lower generation dendrimers.

It can be hazardous to attempt to quantitate the relative amounts of two different species by comparing the intensities of peaks in MALDI/TOF mass spectra. This is especially true when the differences in mass are large. Nevertheless, we can still compare their content qualitatively or semiquantitatively by assuming that all mass fragments have the same response from the mass detector. When two species have similar chemical structures and molecular weights, this assumption is valid. On the basis of this assumption, we find from the spectra that the perfect structure is the most populous species present in these dendrimers; the amount of imperfect dendrimer species present is much smaller.

The relative intensity relationship between the fragment peaks not only proves that our mass assignments are correct but also proves the assumption that the impurities in the dendrimers are caused by the statistical defect mechanism, with some exceptions. For example, since the curve representing missing even numbers of branches is located above the curve representing missing odd numbers of branches, this shows that there is a greater tendency for even numbers of missing branches. In other words, if one branch is missing from an amine, it is also more likely that a second branch will be missing from the same amine. For a purely statistical process one would expect to see fewer species with two defects than with one defect. When two branches are missing, the dendrimer is more likely to consist of structures as shown in Figure 2-4 rather than those shown in Figure 2-5. In addition, $^{7}/_{8}$, $^{3}/_{4}$, and $^{1}/_{2}$ dendrimers are abundant relative to the other impurities.

MALDI/TOF Mass Spectra of DSM Dendrimers of Different Generations after Fractionation. The molecular weight distributions of highly polydisperse samples are usually not accurately measured by MALDI/TOF/MS. In such cases, the molecular weight distribution obtained from MALDI/TOF/MS is much smaller than the distribution obtained from SEC.[16] In many instances for such specimens substantially different

Table 2. Peak Assignments for CN-32 Dendrimer[a]

no. of arms missed	theoretical mass	H^+ peak	relative intensity	Na^+ peak	relative intensity	K^+ peak	relative intensity
0	3384.9	3386.4	100	3408.4	65.3	3425.1	43.4
1	3331.8	3332.8	23.3	3355.4	12.7	3372.0	7.6
2	3274.7	3276.3	29.7	3297.2	18.9	3315.2	10.4
3	3221.6	3223.2	11.8	3244.9	7.7	3262.4	6.5
4	3164.5	3166.3	10.0	3187.9	6.7	3210.1	5.5
5	3111.5	3112.4	2.9	3135.0	2.1	3153.5	1.9
6	3054.4	3056.7	7.6	3078.8	4.2	3096.4	2.9
7	3001.3	3003.2	10.6	3023.8	4.9	3041.7	6.1
8	2944.2	2946.5	4.0	2967.2	3.6	2984.7	2.4

[a] Values based on single measurements.

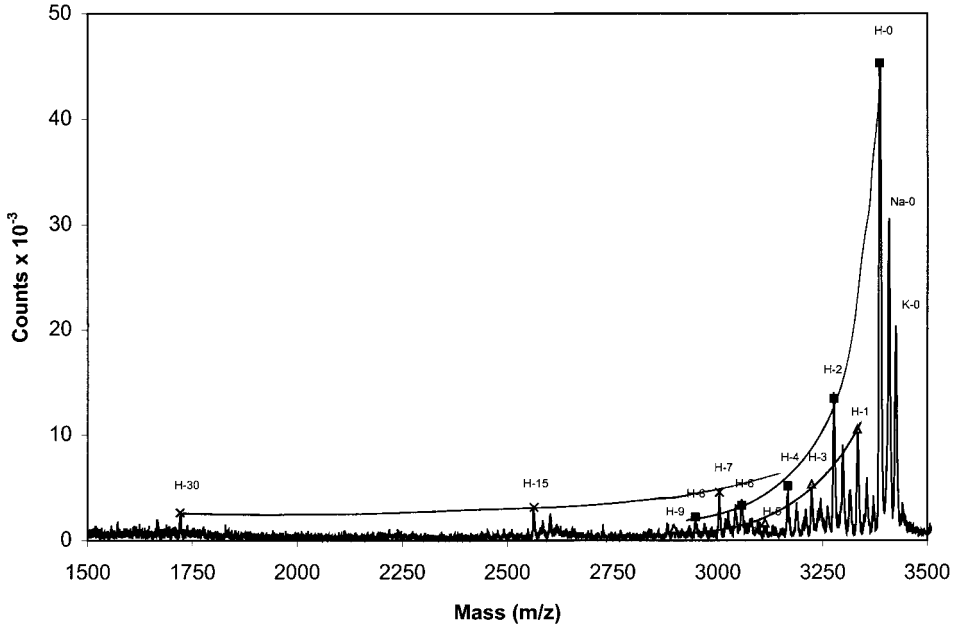

Figure 3. MALDI/TOF/MS peak assignments of CN-32.

molecular weight distributions can be obtained for the same sample spotted on the same well but analyzed under different experimental conditions. On the other hand, under normal conditions it is impractical to determine the molecular weights and molecular weight distributions of dendrimers by means of conventional SEC. The reasons will vary for specific dendrimers systems, but a key factor is the lack of dendritic SEC calibration standards. The condensed molecular architecture of dendrimers causes a large difference in their hydrodynamic volume compared to linear or lightly branched polymers having the same molecular weight. Branched macromolecules of identical size can have different molecular weights depending on the degree of branching and the branching architecture. The SEC universal calibration method cannot be applied, in general, since some dendrimers exhibit a nonlinear relationship between viscosity and molecular weight, and the universal calibration method may or may not be applicable.[17] In this work, we used a SEC fraction collector to collect samples for MALDI/TOF/MS experiments. Each fraction was collected over a period of 30 s. The instrument was configured so that peak broadening was minimized, as tested by a monodisperse organic compound.

SEC behavior of these DSM dendrimers is shown in Figure 4. The chromatograms exhibit broad and tailing peaks. MALDI/TOF/MS spectra of the collected fractionations from peak head to peak tail show that, even though SEC chromatograms are very broad, the molecular weights of the main peaks of different fractions are the same (Figure 5). Comparing the mass spectra of the peak head and peak tail fractions, we find that there is a small amount of dendrimer with double the molecular weight of the main peak in the peak "head fraction" (high molecular weight fraction) and half the molecular weight of the main peak in the peak "tail fraction" (low molecular weight fraction). These are not doubly charged species present in the spectrum corresponding to the tail fraction, since this peak is not observed in the

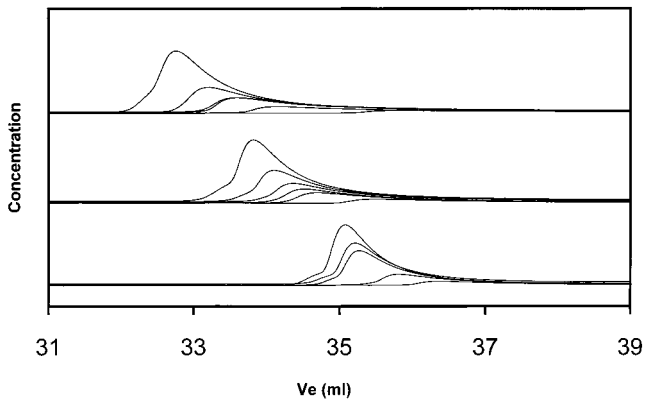

Figure 4. SEC chromatograms of DSM dendrimers in pure THF. From top to bottom, there are three groups of spectra representing respectively CN-64, CN-32, and CN-16. The different peak heights represent different concentrations of each group.

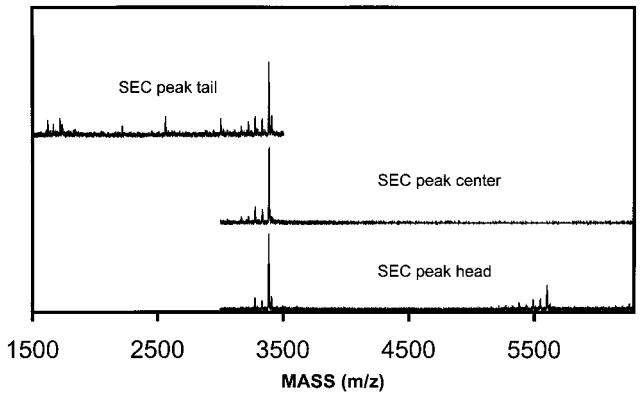

Figure 5. MALDI/TOF/MS spectra of SEC fractions of CN-32. From top to bottom, the spectra show the peak tail, peak center, and peak head fractions.

spectrum for the head fraction, generated under the same experimental conditions. The component of twice the molecular weight observed in the head fraction is not believed to be a dimer produced in the mass spectrometer because a similar peak is not found in the spectrum for the tail fraction, which was generated under the same experimental conditions. These findings strongly suggest that other factors, in addition to molecular weight, are affecting the separation under the SEC conditions employed.

SEC Adsorption Effects. Since the dendrimers are narrowly distributed in molecular weight, peak broadening and tailing in the dendrimer chromatograms could be caused by overloading of the columns. Such overloading, also referred to as "concentration effects", has been attributed to the decrease in hydrodynamic volumes of solvated polymers with increasing concentration and to redistribution phenomena caused by the increased viscosity brought about by the introduction of polymers into the SEC system.[18,19] After injection of a series of solutions with different concentrations, we found that the higher the concentration, the lower the peak tailing and retention volume. This strongly suggests that overloading is not the major cause of distorted peaks. The apparent molecular weight distribution, calculated from the narrowest peak in the chromatograms, suggests that the dendrimers have *broad* molecular weight distributions, which is not supported by MALDI/TOF/MS data. Another possible explanation for the distorted peaks is adsorption of dendrimer on the SEC columns, since the dendrimers contain tertiary amine and cyano groups. We added 1% acetonitrile to the THF mobile phase and repeated the SEC measurements (Figure 6). The tailing phenomenon was not suppressed under these conditions. This suggests that the cyano end groups on the dendrimer molecules do not contribute to the adsorption. When 1% triethylamine was added, however, the peak tailing disappeared, and normal SEC peaks were obtained at all measured concentrations (Figure 7). These findings strongly suggest that column overloading is not the major cause of the peak broadening, which is instead caused by adsorption of tertiary amine groups in the dendrimers onto the SEC columns. It is well-known that polymers containing tertiary amine groups, such as poly(vinylpyridine), exhibit such tailing phenomena in SEC and that the tailing is suppressed by addition of a tertiary amine to the mobile phase. Parts a, b, and c of Figure 8 show SEC elution behavior as a function of concentration for CN-16, CN-32, and CN-64, respec-

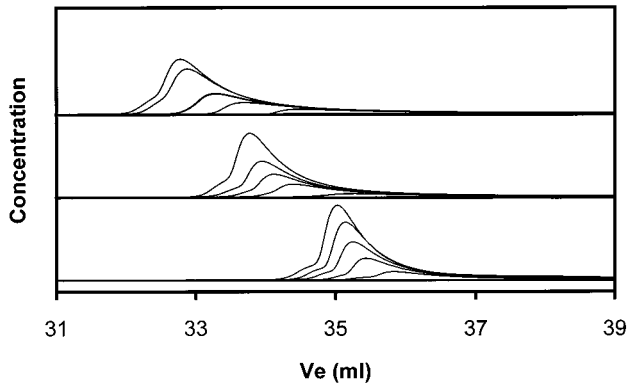

Figure 6. SEC chromatograms of DSM dendrimers at different concentrations in THF with added 1% acetonitrile. From top to bottom, the groups of spectra represent respectively CN-64, CN-32, and CN-16.

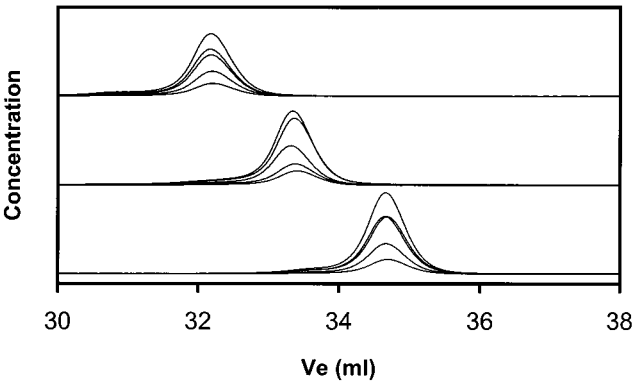

Figure 7. SEC chromatograms of DSM dendrimers at different concentrations in THF with added 1% triethylamine. From top to bottom, the three groups of spectra represent respectively CN-64, CN-32, and CN-16.

tively. From these plots, we see that the curves obtained in the presence of acetonitrile almost overlap with those obtained in pure THF, and the elution volume decays exponentially with increasing concentration. This is because at low concentrations there is a higher relative surface area of the stationary phase per solute molecule. Thus, adsorption effects are enhanced. The flat lines at the bottoms of Figure 8a−c are the SEC peak positions when 1% triethylamine was added to the mobile phase. Since the adsorption was suppressed, the elution volume decreased dramatically. (The changes in thermodynamic quality of mobile phase caused by the addition of 1% of triethylamine should be negligible and should not have much impact on the hydrodynamic volume of the dendrimers.) This phenomenon indicates clearly that tertiary amine groups inside the dendrimers (not the end groups) interact with styragel-type SEC columns and cause adsorption.

Hydrodynamic Radius of the DSM Dendrimers. The dimensions of these same dendrimers have been measured by Scherrenberg and co-workers via small-angle neutron scattering (SANS) and viscometry.[20,21] They found that there is a linear relationship between the generation number and the cube root of molecular weight ($M^{1/3}$). Except for SANS, direct measurement of radius of gyration of dendrimers by traditional methods such as time-averaged light scattering is extremely difficult since the size of dendrimers is normally below the lower detection limit of the method. There are, however, two simple methods that can be used to estimate the size of the dendrimers. One is dilute

Table 3. Intrinsic Viscosity and Hydrodynamic Radius of DSM Dendrimers with Cyano End Groups

	M	$[\eta]$,[a] dL/g	K_H[b]	R_h,[c] nm	$[\eta]$,[d] dL/g	k_H[e]	R_h,[f] nm	R_h,[g] nm	$[\eta]$,[h] dL/g	R_h,[i] nm	R_g,[j] nm	R_h,[k] nm
CN-16	1622	0.0351	1.87	0.968	0.0363	1.39	0.977	0.950	0.034	0.960	0.800	1.02
CN-32	3385	0.0363	2.20	1.25	0.0383	1.45	1.27	1.23	0.035	1.23	1.01	1.29
CN-64	6910	0.0380	2.28	1.61	0.0400	1.50	1.64	1.73	0.036	1.58	1.22	1.56

[a] Intrinsic viscosity from first-order fit. [b] Huggins coefficient from first-order fit. [c] Hydrodynamic radius calculated from first-order fitted intrinsic viscosity data. [d] Intrinsic viscosity from second-order fit. [e] Huggins coefficient from second-order fit. [f] Hydrodynamic radius calculated from second-order fitted intrinsic viscosity data. [g] Hydrodynamic radius calculated from SEC results. [h] Intrinsic viscosity measured in acetone by Scherrenberg.[20] [i] Hydrodynamic radius calculated from intrinsic viscosity in acetone by applying hard-sphere model. [j] Radius of gyration, R_g, measured by small-angle neutron scattering (SANS) in acetone-d_6 by Scherrenberg.[20] [k] Hydrodynamic radius calculated from R_g[20] by applying the hard-sphere model[24] (assumes R_h/R_g is equal to 1.28).

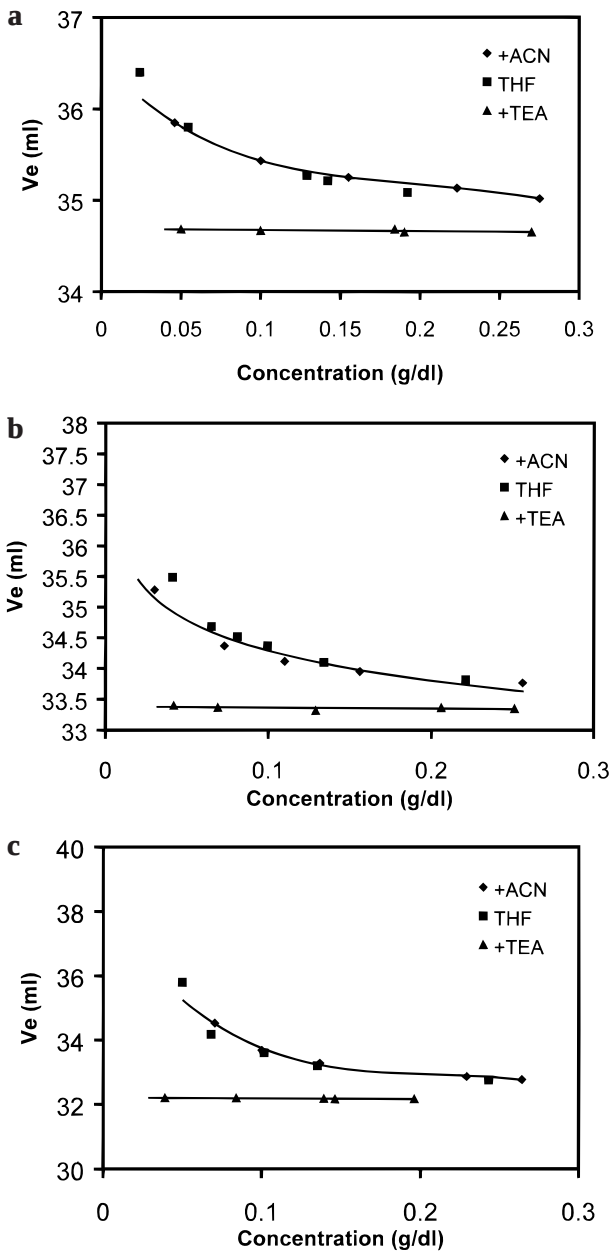

Figure 8. Shift of SEC peaks caused by the different concentrations of (a) CN-16, (b) CN-32, and (c) CN-64.

solution viscometry, and the other is SEC universal calibration.

Intrinsic Viscosity Method. The intrinsic viscosity of the dendrimers was measured using Huggins equation,

$$\eta_{sp}/C = [\eta] + k_{H_1}[\eta]^2C + k_{H_2}[\eta]^3C^2 + \ldots \qquad (2)$$

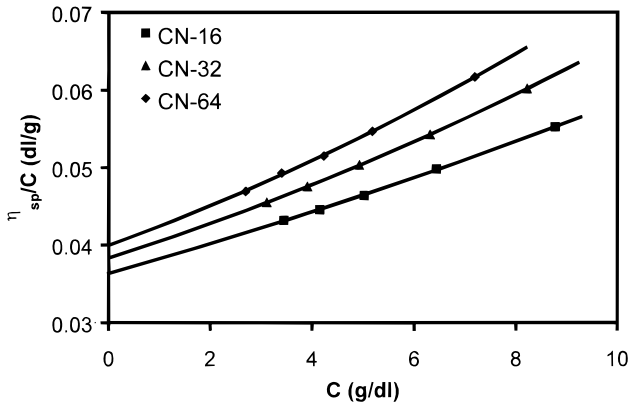

Figure 9. Second-order fits to viscosity data obtained for DSM dendrimers.

where K_{H_1} and K_{H_2} are the first- and second-order concentration coefficients, and K_{H_1} is usually referred to as the Huggins coefficient. From the experimental data, we find that a second-order Huggins equation must be used to fit the data, since all the data sets exhibit curvature (Figure 9). Comparing the results obtained from first- and second-order fitting (Table 3), we find that linear extrapolation gives systematically lower $[\eta]$ and higher Huggins coefficients. Second-order fitting yields Huggins coefficients of 1.4−1.5 for the DSM dendrimers. Since dendrimers are spherelike objects, it is interesting to compare our Huggins coefficients with theoretical and experimental values for spheres and other spherelike objects (multiarmed star polymers). K_{H_1} is predicted by Batchelor [22] to have a value of 0.99 for hard spheres. The 18-arm and higher arm polyisoprene stars were found to exhibit "fuzzy sphere" behavior in both good solvents and Θ solvents.[23] The Huggins coefficients for these materials ranged from 0.6 to 9.2, with most values close to unity in reasonable accord with our data from second-order fits. Since first-order fitting gives much higher Huggins coefficients, we believe that second-order fits are more reliable.

The hydrodynamic radius, R_h, can be calculated from the intrinsic viscosity by applying the Einstein hard-sphere equation,

$$R_h = [3M[\eta]/10\pi N_a]^{1/3} \qquad (3)$$

where M is the molecular weight and N_a is the Avogadro's number. By plotting log $[\eta]$ and log R_h versus log M, we find that both relationships are linear (Figures 10 and 11; Table 3).

The slope of the log M versus log $[\eta]$ plot, α of the Mark−Houwink−Sakurada (MHS) equation, is very small. The reason for this small slope is that molecular weight is exponentially proportional to the generation

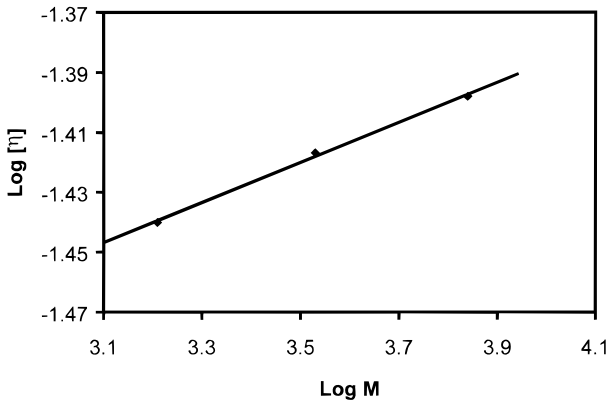

Figure 10. Double-logarithmic plot of intrinsic viscosity versus molecular weight.

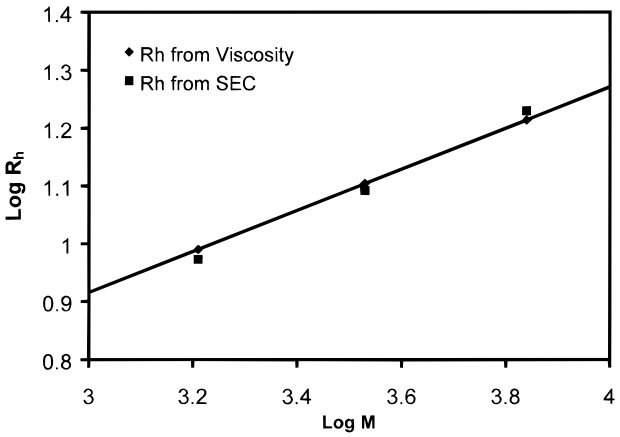

Figure 11. Double-logarithmic plot of hydrodynamic radius versus molecular weight.

number but size is linearly proportional to the generation number for dendrimers. The double-logarithmic representation of R_h versus the molecular weight for the dendrimer gives a linear relationship with a slope of 0.356. The linear relationships of log [η] and R_h versus log M indicate that the density of the solvated dendrimer does not change much for the different generations. The exponent of R_h is close to the limiting case $R \propto M^{1/3}$ for hard-spheres structure.[12] De Brabander-van den Berg [25] reported that intrinsic viscosity of these cyano-terminated dendimers (generations 1−5) reaches a maximum, at generation 4, as a function of generation number. Our intrinsic viscosity measurements on generation 3, 4, and 5 Astramol dendrimers fail to confirm this phenomenon. Our viscosity values are very close to those measured by Scherrenberg and co-workers[20] for the same dendrimers in acetone (Table 3); these authors also failed to find a maximum in [η] up to generation 5, in accord with our data. As predicted in recent theoretical work, the intrinsic viscosities of dendrimers do not necessarily exhibit a maximum as the function of generation number.[26]

Universal Calibration Method. From the SEC peak elution volumes, we can estimate the hydrodynamic radii of the dendrimers on the basis of the universal calibration concept. To do so, we assume that the hydrodynamic volume of dendrimers is the same as the hydrodynamic volume of polystyrene (PS) at a given elution volume. From the calibration curve we can calculate the molecular weight of the PS corresponding to that elution volume. Then the hydrodynamic volume can then be calculated from the relationship between molecular weight and hydrodynamic volume of PS.[27] From this hydrodynamic volume versus elution volume relationship, the hydrodynamic radius of the dendrimer may be calculated since molecular weight is known from MALDI/TOF/MS. The results are shown in Figure 11 and Table 3.

From Figure 11, we can see that the hydrodynamic radii from the universal calibration method agree very well with those obtained via the intrinsic viscosity method. This supports the validity of SEC universal calibration for this class of dendritic macromolecules. Also, results from viscosity and universal calibration method agree well with the SANS[20] results shown in Table 3.

Conclusions

MALDI/TOF/MS combined with SEC fraction collection makes it possible to study the molecular weight, molecular weight distribution, and structure of dendrimers. Compared with SEC and other traditional methods for polymer molecular weight characterization, MALDI/TOF/MS offers much higher mass accuracy and resolution, provided molecular weight is not too high. In this work, imperfect dendrimers were distinguished from the main (perfect) dendritic products based upon mass accuracies of 1−3 Da, depending on molecular weight. On the basis of their masses, the structures of virtually all of the imperfect species could be assigned. There was no evidence to suggest the presence of cyclic (type 2) defects in these materials. Combined MALDI/TOF/MS and SEC methods can also be used to determine molecular weight distributions of dendrimers. Combined SEC and viscometry results for poly(ethyleneimine) dendrimers having cyano end groups and covering generations 3−5 provide strong evidence that these dendrimers have compact structures. Nevertheless, tertiary amine groups in these dendrimers are able to interact strongly with the polystyrene-based stationary phase during SEC experiments in THF. Adsorption was suppressed by adding tertiary amine to the mobile phase. No peak in intrinsic viscosity was observed as a function of dendrimer generation up to generation 5.

Acknowledgment. This research was supported by the U.S. Army Research Office through its DURIP Program (DAAG55-97-1-0075).

References and Notes

(1) Tomalia, D. A.; Naylor, A. M.; Goddard, W. A., III *Angew. Chem., Int. Ed. Engl.* **1990**, *29*, 138.
(2) Newkome, G. R.; Moorefield, C. N.; Baker, G. R. *Aldrichim. Acta* **1992**, *25*, 31.
(3) Hawker, C. J.; Fréchet, J. M. J. *J. Am. Chem. Soc.* **1990**, *112*, 7638.
(4) Voit, B. I. *Acta Polym.* **1995**, *46*, 87.
(5) Malmström, E.; Hult, A. *J. Macromol. Sci., Rev. Macromol. Chem. Phys.* **1997**, *C37*, 555.
(6) Bosman, A. W.; Jansenn, H. M.; Meijer, E. W. *Chem. Rev.* **1999**, *99*, 1665.
(7) Matthews, O. A.; Shipway, A. N.; Stoddart, J. F. *Prog. Polym. Sci.* **1998**, *23*, 1.
(8) Koper, G. J. M.; van Genderen, M. H. P.; Elissen-Roman, C.; Baars, M. W. P. L.; Meijer, E. W.; Borkovec, M. *J. Am. Chem. Soc.* **1997**, *119*, 6512.
(9) Fréchet, J. M. J.; Lochmann, L.; Šmigol, V.; Švec, F. *J. Chromatogr., A* **1994**, *667*, 284.
(10) Bauer, B. J.; Topp, A.; Prosa, T. J.; Amis, E. J. *Polym. Mater. Sci. Eng.* **1997**, *77*, 87.
(11) Mansfield, M. L.; Klushin, L. I. *J. Phys. Chem.* **1992**, *86*, 3994.
(12) Murat, M.; Grest, G. S. *Macromolecules* **1996**, *29*, 1278.

(13) La Ferla, R. J. *Chem. Phys.* **1997**, *106*, 678.
(14) Chai, C.; Chen, Z. Y. *Macromolecules* **1997**, *30*, 5104.
(15) Hummelen, J. C.; van Dongen, J. L. J.; Meijer, E. W. *Chem. Eur. J.* **1997**, *3*, 1489.
(16) Lehre, R. S.; Sarson, D. S. *Rapid Commun. Mass Spectrom.* **1995**, *9*, 91.
(17) Mourey, T. H.; Turner, S. R.; Rubinstein, M.; Fréchet, J. M. J.; Hawker, C. J.; Wooley, K. L. *Macromoecules* **1992**, *25*, 2401.
(18) Yamakawa, H. *J. Chem. Phys.* **1965**, *43*, 1334.
(19) Mahabadi, H. K.; Rudin, A. *Polym. J.* **1979**, *11*, 123.
(20) Scherrenberg, R.; Coussens, B.; van Vliet, P.; Edouard, G.; Brackman, J.; de Brabander, E. *Macromolecules* **1998**, *31*, 456.
(21) Ramzi, A.; Scherrenberg, R.; Brackman, J.; Joosten, J.; Mortensen, K. *Macromolecules* **1998**, *31*, 1621.
(22) Batchelor, G. K. *J. Fluid Mech.* **1977**, *83*, 97.
(23) Bauer, B. J.; Fetters, L. J.; Graessley, W. W.; Hadjichristidis, N.; Quack, G. F. *Macromolecules* **1989**, *22*, 2337.
(24) Yamakawa, H. *Helical Wormlike Chains in Polymer Solution*; Springer: Berlin, 1997.
(25) de Brabander-van den Berg, E. M. M.; Meijer, E. W *Angew. Chem., Int. Ed. Engl.* **1993**, *32*, 1308.
(26) Cai, C.; Chen, Z. Y. *Macromolecules* **1998**, *31*, 6393.
(27) Fetters, L. J.; Hadjichristidis, N.; Lindner, J. S.; Mays, J. W. *J. Phys. Chem. Ref. Data* **1994**, *23*, 619.

MA990458P